

CONFERENCES AND SYMPOSIA

PACS numbers: 01.10.Fv, **42.25. – p**, **42.30. – d**, 42.60.Jf, 72.80.Vp, **73.20. – r**, **75.30. – m**, **75.50. – y**, 81.05.Bx, 81.05.ue

Modern problems in physical sciences
(Scientific session of the Physical Sciences Division of the Russian Academy of Sciences, 26 October 2011)

DOI: 10.3367/UFNe.0182.201204d.0437

A scientific session of the Physical Sciences Division of the Russian Academy of Sciences (RAS) was held in the conference hall of the P N Lebedev Physical Institute, RAS on 26 October 2011.

The following reports were put on the session's agenda posted on the website www.gpad.ac.ru of the RAS Physical Sciences Division:

(1) **Morozov S V** (Institute of Microelectronics Technology and High Purity Materials, RAS, Chernogolovka, Moscow region) "New effects in graphene with high carrier mobility";

(2) **Volostnikov V G** (Samara Branch of the P N Lebedev Physical Institute, RAS, Samara) "Modern optics of Gaussian beams";

(3) **Mushnikov N V** (Institute of Metal Physics, Ural Branch of the Russian Academy of Sciences, Ekaterinburg) "Intermetallide-based magnetic materials".

The papers written on the base of these reports are published below.

PACS numbers: 72.80.Vp, **73.20. – r**, 81.05.ue
DOI: 10.3367/UFNe.0182.201204e.0437

New effects in graphene with high carrier mobility

S V Morozov

1. Ways of improving mobility and ballistic transport in graphene

The study of graphene is among the most rapidly advancing areas of solid-state physics. Graphene continues to surprise physicists with its various properties, combining a high strength, record high extensibility, and high conductivity, thermal conductivity, optical transparency, etc. But the chief thing attracting the attention of numerous researchers to graphene is its unusual electronic system and unique transport properties [1–5].

Carriers in graphene have exhibited a rather high mobility, even in the early experimental works, despite the fact that a film only one atom in thickness was in no way protected from the environment. It is significant that the high carrier mobility persisted upon increasing the temperature to room temperature owing to relatively weak electron–phonon scattering. However, attempts to raise the mobility to values exceeding the typical values of $(1-2)\times10^4$ cm^2 V^{-1} s^{-1} observed in graphene on oxidized silicon substrates did not meet with success for a long time. The scattering by nanowavy film structure and more recently the scattering by resonant impurities were considered as the main scattering mechanisms responsible for limiting electron mobility in graphene [2, 3].

A new stage in the study of graphene commenced with the emergence of structures exhibiting a far higher (by 1–2 orders of magnitude) mobility. It became clear that the new structures made it possible to study many subtle multiparticle effects, in particular, the fractional quantum Hall effect which was discovered in the new structures [6].

This report reviews the experiments on high-mobility graphene structures, which were recently performed by the author jointly with A Geim's group at the University of Manchester.

Two ways of obtaining more perfect graphene structures began to show: the use of suspended bridges, and encapsulation of graphene between boron nitride (BN) crystallites. The former method involves the making of graphene bridges suspended between metal contacts (Fig. 1a). First, the standard method of micromechanical delamination is employed to fabricate graphene bridges on an oxidized silicon substrate. Then, a part of the oxide under the graphene bridge is removed by chemical etching. An important role is played by the concluding annealing of the structure with the help of current pulses passed through the suspended graphene bridge. The annealing is executed under conditions close to the threshold of bridge damage; however, it permits attaining locally high temperatures (estimated at 700–800 °C) without degrading the remaining parts of the structure. Our experience suggests that long-term exposure of graphene structures on silicon oxide to temperatures above 400 °C impairs the transport properties of graphene.

S V Morozov Institute of Microelectronics Technology and High Purity Materials, Russian Academy of Sciences, Chernogolovka, Moscow region, Russian Federation
E-mail: morozov@iptm.ru

Uspekhi Fizicheskikh Nauk **182** (4) 437 – 455 (2012)
DOI: 10.3367/UFNr.0182.201204d.0437
Translated by E N Ragozin, E G Strel'chenko; edited by A Radzig

Uspekhi Fizicheskikh Nauk **182** (4) 437 – 442 (2012)
DOI: 10.3367/UFNr.0182.201204e.0437
Translated by E N Ragozin; edited by A Radzig

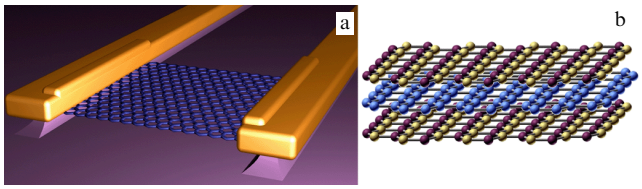

Figure 1. (a) Suspended graphene bridge. (b) Graphene encapsulated between two-dimensional crystals of boron nitride.

This technique permits attaining record high mobility in graphene (above 10^6 cm^2 V^{-1} s^{-1}), but at the same time leads to several disadvantages. First, this technique permits fabricating structures which are highly limited in both the size (typically micrometer-sized) and topology (ordinarily only two-contact structures). Second, suspended graphene structures are in no way protected from the environment as before and the concluding annealing is carried out directly in a low-temperature cryostat in an inert helium atmosphere.

The second way of obtaining high-mobility structures consists in placing graphene between thin (down to monolayer-thin) crystallites of boron nitride (Fig. 1b).

From a more general viewpoint, the latter way of constructing graphene–boron nitride layered structures exhibits a way of fabricating three-dimensional crystals on the base of different two-dimensional constituents. There are different approaches to the formation of new quasi-two-dimensional graphene-based crystals. The feasibility of obtaining new quasi-two-dimensional crystals by chemical modification of graphene has been demonstrated in recent years. This method was employed to obtain graphan [7] and fluorographene [8], in which hydrogen and fluorine atoms, respectively, are attached to the graphene lattice in an ordered manner. Graphan and fluorographene possess dielectric properties, and may be recovered to the initial graphene on thermal processing.

Earlier, we showed [9] that the capacity of forming two-dimensional crystals is inherent not only in carbon and that they may be produced also from other layered materials, like boron nitride, high-temperature superconducting BiSCCO ceramics, and some dichalcogenides. Therefore, the spectrum of two-dimensional crystals is rather broad: from semimetals to dielectrics and superconductors. By placing individual monolayers of different two-dimensional crystals one on top of the other, it is basically possible to obtain new heterostructures with highly diverse properties.

One of the first examples of the implementation of such heterostructures is the encapsulation of graphene between two-dimensional boron nitride crystals with an atomic-smooth surface, which were obtained by micromechanical delamination. The fabrication procedure of the like structures comprises the following stages. First, thin crystallites of boron nitride are placed on the surface of oxidized silicon with the aid of micromechanical delamination. A graphene film is formed in a similar manner on another oxidized silicon substrate preliminarily coated with a polymer. Next, the graphene on the polymer is transferred to the first substrate and superposed with the BN crystallite. On dissolving the polymer, forming the topology of the structure, and metallization routing, the structure is covered with another boron nitride film.

Both methods described above have advantages and disadvantages of their own. Today, the highest electron mobility in suspended graphene bridge structures exceeds 10^6 cm^2 V^{-1} s^{-1}. At the same time, suspended bridges are seriously limited in size as well as in structure topology, which is due to the complexity of their annealing by current pulses, while the two-point measurement system significantly bounds the scope of possible investigations. The graphene on BN is devoid of these drawbacks, since the encapsulation of graphene protects it to a large extent from the action of the environment, but the magnitudes of mobility attained to date have been somewhat lower [as a rule, no greater than $(1-2)\times10^5$ cm^2 V^{-1} s^{-1}].

The advent of high-mobility graphene structures based on boron nitride made it possible to explicitly demonstrate ballistic transport [10]. The experiment was carried out on Hall bridges in the geometry of bend resistance $R_B = V_{34}/I_{21}$ (see the inset to Fig. 2). The current flows between contacts 2 and 1, while the potential difference is measured across contacts 3 and 4, which may be calculated by Van der Pau's formula for the case of diffusion transport. The bend resistance in high-mobility structures is negative in a wide carrier density range, with the exception of a low-concentration domain, testifying that the injected carriers pass from contact 2 to contact 4 almost without scattering (ballistically). A similar effect has earlier been demonstrated in high-mobility GaAlAs heterostructures, and its realization requires that the carrier free path far exceed the characteristic dimensions of the active region of the structure [11]. On application of a weak magnetic field perpendicular to the graphene layer, the bend resistance R_B becomes positive (see Fig. 2), because the magnetic field bends the trajectories of injected electrons and they can no longer reach the opposite contact ballistically. With the assumption of diffuse carrier scattering from the specimen's boundaries, it is possible to estimate the free path in the film bulk: it is ~ 3 μm at helium temperature, and ~ 1.5 μm at room temperature. Therefore, graphene–BN heterostructures exhibit micrometer-scale ballistic transport even at room temperature, which undoubtedly opens up new vistas for the development of high-frequency, low-noise microelectronic applications.

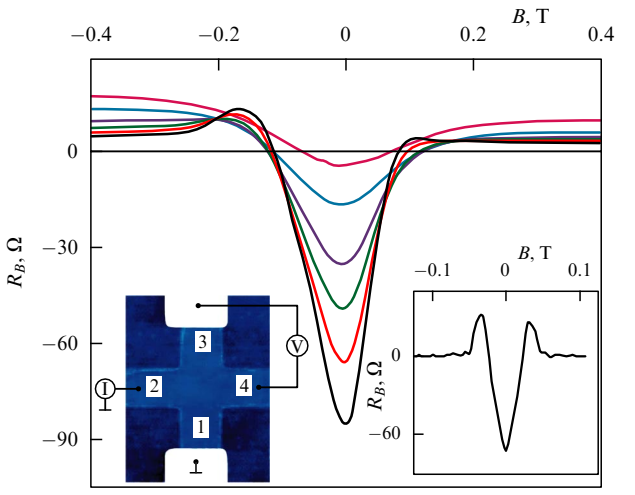

Figure 2. Bend resistance $R_B = V_{34}/I_{21}$ as a function of magnetic field B for $n \approx 6\times10^{11}$ cm^{-2} and temperatures of 50, 80, 110, 140, 200, and 250 K (from the lowermost curve to the topmost one, respectively). The inset at the left shows the measurement schematic, and the inset at the right depicts the calculated dependence $R_B(B)$ for $n \approx 6\times10^{11}$ cm^{-2} in the billiards model [11].

2. Features of the band structure in the vicinity of the electroneutrality point

A high carrier mobility is one of the principal special features of new specimens, though far from being the only one. A wealth of interesting physical effects are expected near the point of electric neutrality (on approaching a zero carrier concentration). But in a real experimental situation, it is hardly possible to reach this point. Indeed, since there are chaotic potential fluctuations, on lowering the carrier concentration the two-dimensional electron gas breaks up into 'pools' with holes and electrons (at points of local rise and fall in the potential, respectively), and therefore a uniform situation with the zero carrier concentration cannot be reached. Of course, how close it is possible to approach the Dirac point depends on the purity and quality of the specimens. New graphene structures have allowed lowering the working carrier concentration by factors of 10–100 and studying the details of the band structure in the vicinity of the electroneutrality point.

First, let us discuss single-layer graphene. The charge carriers in graphene are similar to relativistic particles with a zero rest mass. The linear dispersion law is described by the expression $E = v_F \hbar k$, where the Fermi velocity v_F plays the part of the speed of light, and k is the wave vector. As the carrier concentration lowers and the electroneutrality point is approached, the screening length increases and the electron–electron interaction plays an increasingly important part. The standard Landau theory of a Fermi liquid, which permits representing a strongly interacting electron liquid as a gas of noninteracting electrons, will no longer be applicable. The inset to Fig. 3 illustrates the form of single-layer graphene spectra obtained in a single-particle approximation using the renormalization group technique [12]. The inclusion of electron–electron interaction results in a lowering of the density of states at low energies and in an increase in v_F, with a logarithmic divergence in concentration near the zero energy.

By measuring the temperature dependences of Shubnikov–de Haas oscillations, it was possible to obtain the dependence of the cyclotron mass on the carrier concentration n [12]. The experimental curve $v_F(n)$ corresponding to the latter dependence is depicted in Fig. 3. In new high-mobility specimens there is a possibility (which did not exist in our earlier work [13]) of varying the carrier concentration within three orders of magnitude. Experimental points show a threefold rise in v_F as the Dirac point is approached, which nicely agrees with the theory. Furthermore, several theoretical papers [14–17] predict that electron–electron interaction at low energies may give rise to new electron phases accompanied by the formation of a forbidden band. However, our experiments revealed no hints at a dielectric behavior of graphene down to energies on the order of 0.1 meV.

An even more interesting picture of the dispersion law at low energies was discovered in two-layer graphene [18]. The single-particle theory [19] predicts that the parabolic dispersion law in two-layer graphene passes into a quasilinear one (the four minicones in the left inset to Fig. 4) for an energy $E < 1$ meV. It was not feasible to ascertain the presence of these special features in standard graphene structures on an oxidized silicon substrate, which had a typical mobility of $\sim 10^4$ cm^2 V^{-1} s^{-1}. However, it was possible to verify the data of theoretical calculations on suspended bridges of two-layer graphene with a mobility of $\sim 10^6$ cm^2 V^{-1} s^{-1}. The behavior of the temperature dependence of resistance and the picture of the motion of Landau levels along energy coordinate when varying the magnetic field (Fig. 4) are indications that the cones with a quasilinear spectrum do exist, but there are only two of them rather than four. It is precisely this picture caused by nematic phase transition with a lowering of rotational symmetry in the electron subsystem of two-layer graphene that is predicted by many-particle theories [20, 21].

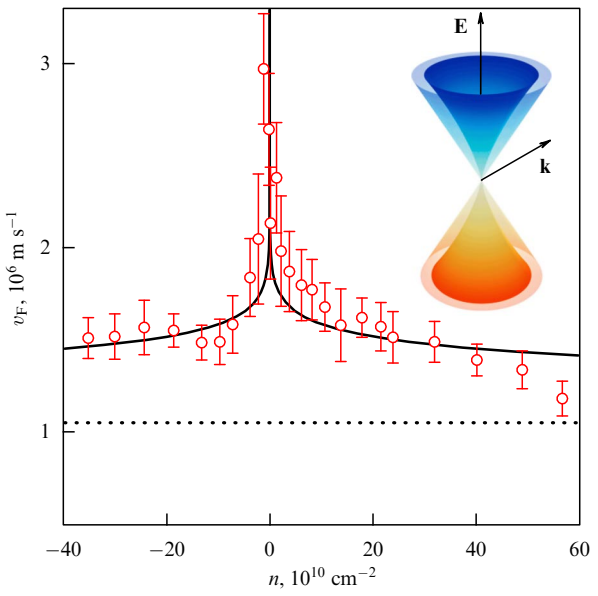

Figure 3. Experimental (circles) and theoretical (solid curve) dependences of Fermi velocity v_F on the charge carrier concentration n in single-layer graphene. The dotted line fits the standard value of v_F in graphene at high concentrations. The inset shows a diagram of the band structure in single-layer graphene at low concentrations without (a single-particle approximation, the outer cone) and with (the inner cone) the inclusion of electron–electron interactions.

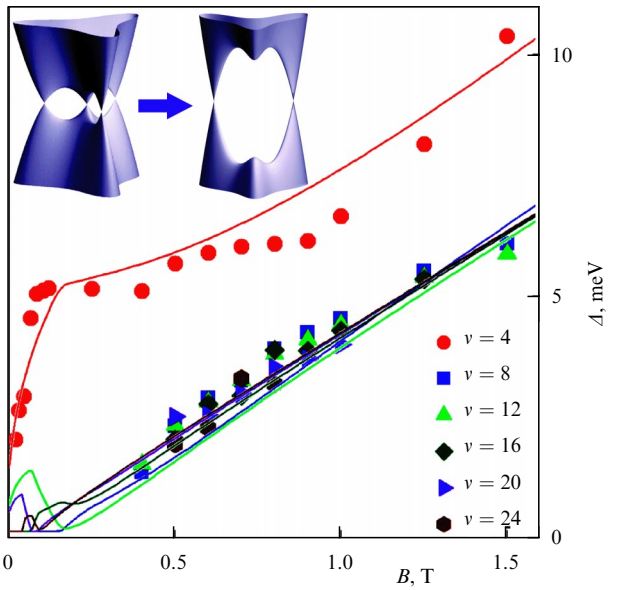

Figure 4. Experimental (symbols) and calculated (curves) dependences of cyclotron gaps Δ for different occupation numbers ν. The inset displays the low-energy portion of the two-layer graphene spectrum in a single-particle approximation (the left part of the inset) and its reconstruction in nematic phase transition (the right part of the inset).

3. Giant spin Hall effect in graphene

The fact that graphene is a semiconductor with a zero band gap revealed itself unexpectedly in nonlocal transport experiments [22]. In the experiment schematized in Fig. 5a, the electric current is passed between the contacts which are quite close to each other, while the potential drop is measured away from the classical current flow path. In a magnetic field, a voltage appeared across remote contacts, whose dependence on the carrier concentration or on the magnetic field was qualitatively similar to the oscillations of longitudinal magnetoresistance. Experiments of this kind had earlier been carried out in high-mobility GaAs heterostructures, and their results were attributed to the edge character of current flow in a quantizing magnetic field and to the scattering of edge states [23, 24]. An advantage of the nonlocal experiment is that it enables filtering out the ohmic contribution in the current flow and detecting more subtle effects.

However, experimental results obtained with graphene significantly depart from those with semiconductors [22]. First, the effect manifests itself with an increase in temperature up to room temperature, and at low temperatures it also takes place in low magnetic fields up to 0.1 T (Fig. 6), making problematic the explanation of experimental data by the scattering of edge states. Second, the effect is much more pronounced only for the zero Landau level (which resides at zero energy).

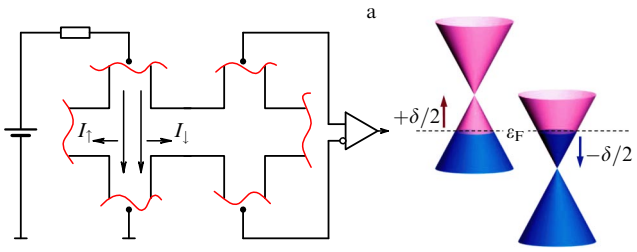

Figure 5. Spin Hall effect in graphene. Schematic of the experiment and an illustration of the emergence of the spin current in a direction perpendicular to the charge current (a) as a result of Zeeman level shifts and the production of electrons and holes with oppositely directed spins in a magnetic field at the electroneutrality point (b).

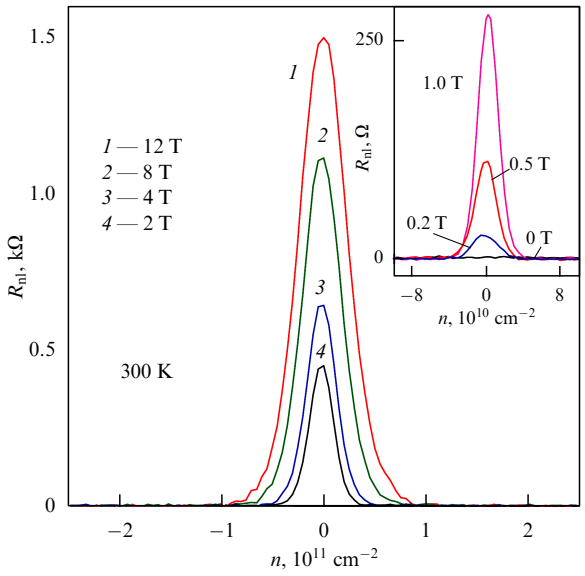

Figure 6. Nonlocal resistance of single-layer graphene encapsulated between boron nitride crystallites in different magnetic fields at room temperature.

The idea of explaining nonlocal response in graphene near the point of electroneutrality is illustrated in Fig. 5b. The Zeeman level splitting in a magnetic field shifts the Dirac cones up and down in energy for quasiparticles with opposite spin directions. When graphene resides at the point of electroneutrality, this gives rise to a finite concentration of electrons and holes with opposite spin directions. In the passage of electric current, the Lorentz force induces the currents of the carriers with opposite spins in the opposite transverse directions, thus leading to a spatial spin disbalance (the spin Hall effect). In this case, the hole and electron charge currents compensate each other in the transverse direction, and the Hall voltage is equal to zero at the point of electroneutrality. Owing to a rather weak spin relaxation [2, 25], a potential drop appears across remote contacts due to inverse transformation.

Phenomenologically, the situation is similar to that for the spin Hall effect caused by spin–orbit interaction [26–28]. The spin–orbit interaction in graphene is weak, and the effect is due to Zeeman level splitting in a magnetic field and the zero band gap. In this case, its magnitude is two orders of magnitude greater than that of the spin Hall effect in conventional semiconductors, which makes the spin Hall effect in graphene quite suited for use in spintronics.

4. Metal–insulator transition in graphene

In the early experimental works on graphene, it came as a surprise that the maximum graphene resistivity ρ near the electroneutrality point approached a value $\propto h/e^2$ (per carrier type), but no indications of strong localization were observed in this case. Indeed, even weak chaotic potential fluctuations in two-dimensional systems lead to a sharp rise in resistivity on lowering the temperature and the carrier concentration [29, 30]. A value of ρ exceeding the quantity h/e^2 signifies that the carrier free path l becomes shorter than the Fermi wavelength λ_F, so that quantum interference begins to play the dominant role, resulting in a strong (Anderson) localization. Because of the thermal activation of the carriers, only a weak temperature dependence of the conductivity was observed, even at the point of electroneutrality in graphene.

The situation changed radically on executing experiments [31] on a system consisting of two closely spaced, but electrically separated, graphene layers with a high mobility ($\sim 10^6$ cm^2 V^{-1} s^{-1}). Figure 7a presents the schematics of the experiment and the multilayer BN–graphene–BN–graphene-BN structure under investigation, which lies on an oxidized silicon plate. Measurements were made of the transport properties of the first (investigated) graphene layer, with the second (control) graphene layer serving as a neighboring gate for the first layer (along with the Si substrate). It is significant that the thickness of the boron nitride layer between the graphene layers was equal approximately to 10 nm, and by varying the carrier concentration in the control graphene layer it was possible to substantially change the screening in the graphene layer under investigation.

At low carrier concentration n_c in the control layer, the graphene layer studied exhibited a usual behavior with a conductivity minimum of $\propto 4e^2/h$. However, for $n_c > 10^{11}$ cm^2 V^{-1} s^{-1} the resistivity rose rapidly near the electroneutrality point at low temperatures (see Fig. 7). In this case, the rise in resistivity was suppressed by a weak

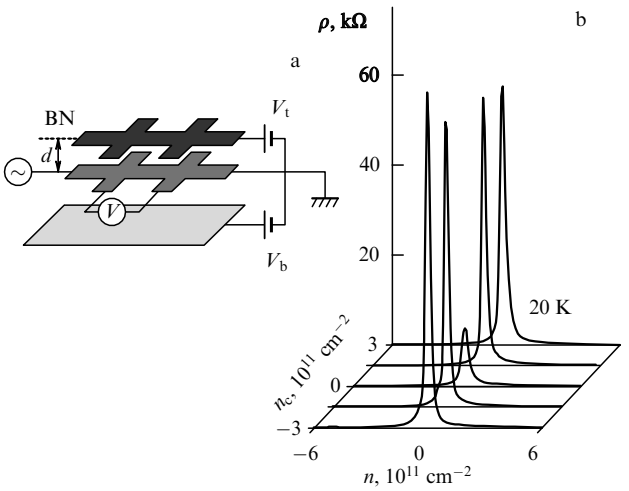

Figure 7. (a) Schematic diagram for the measurement in a structure comprising two separated graphene layers lying on an oxidized silicon substrate (the lower layer). There are boron nitride crystallites (not shown in the drawing) between all the layers. The thickness of the boron nitride layer between the graphene layers is $d \approx 10$ nm. (b) Dependence of the resistivity ρ on the carrier concentration n in the graphene layer under investigation for different carrier concentrations n_c in the control (upper) graphene layer.

magnetic field ($B < 0.1$ T) perpendicular to the graphene layer, which is more likely an indication of an interference effect rather than of the discovery of a forbidden band in graphene.

This behavior of the resistivity is indicative of a metal–insulator transition, demonstrating the Anderson localization on increasing $\rho > h/e^2$. In standard specimens on a silicon substrate, the metal–insulator transition is masked by inhomogeneities and the formation of 'pools' of electrons and holes near the electroneutrality point. The state of graphene inside each of them is far from electroneutrality point, and it remains metallic. Accordingly, the resistivity of the system is determined by semitransparent (owing to Klein tunneling [32, 33]) electron–hole transitions with a weak temperature dependence [34, 35].

The control graphene layer may effectively screen the fluctuation potential and suppress the emergence of electron and hole pools, making it possible to study the behavior of graphene in the vicinity of the electroneutrality point. This interpretation also favors the idea that the proximity of the minimal conductivity in traditional structures to the quantity $4e^2/h$ is due to the flow across the boundaries of the pools of electrons and holes. Therefore, an unusual situation, which is extrinsic to conventional metals and semiconductors, is realized in graphene, whereby localization results from a lowering of disordering rather than from its increasing.

In summary, it should be noted that the emergence of high-mobility graphene structures has led not only to a refinement of certain notions of the graphene physical properties, but also to their revision. At the same time, it is hard to overestimate the promise of the recently commenced work on layered structures consisting of two-dimensional crystals of boron nitride and graphene.

Graphene began its history at some point by separating from its three-dimensional progenitor — graphite. It is not unlikely that in the near future we will obtain a variety of new three-dimensional materials custom-made of different two-dimensional crystals and highly diversified in properties.

Acknowledgments. This work was supported by the Russian Foundation for Basic Research and the Programs of the Presidium of the Russian Academy of Sciences which are gratefully acknowledged.

References

1. Geim A K, Novoselov K S *Nature Mater.* **6** 183 (2007)
2. Castro Neto A H et al. *Rev. Mod. Phys.* **81** 109 (2009)
3. Das Sarma S et al. *Rev. Mod. Phys.* **83** 407 (2011)
4. Lozovik Yu E, Merkulova S P, Sokolik A A *Usp. Fiz. Nauk* **178** 757 (2008) [*Phys. Usp.* **51** 727 (2008)]
5. Morozov S V, Novoselov K S, Geim A K *Usp. Fiz. Nauk* **178** 776 (2008) [*Phys. Usp.* **51** 744 (2008)]
6. Dean C R et al. *Nature Phys.* **7** 693 (2011)
7. Elias D C et al. *Science* **323** 610 (2009)
8. Nair R R et al. *Small* **6** 2877 (2010)
9. Novoselov K S et al. *Proc. Natl. Acad. Sci. USA* **102** 10451 (2005)
10. Mayorov A S et al. *Nano Lett.* **11** 2396 (2011)
11. Beenakker C W J, van Houten H *Phys. Rev. Lett.* **63** 1857 (1989)
12. Elias D C et al. *Nature Phys.* **7** 701 (2011)
13. Novoselov K S et al. *Nature* **438** 197 (2005)
14. Bostwick A et al. *Science* **328** 999 (2010)
15. Khveshchenko D V *Phys. Rev. Lett.* **87** 246802 (2001)
16. Gorbar E V et al. *Phys. Rev. B* **66** 045108 (2002)
17. Drut J E, Lähde T A *Phys. Rev. Lett.* **102** 026802 (2009)
18. Mayorov A S et al. *Science* **333** 860 (2011)
19. McCann E, Fal'ko V I *Phys. Rev. Lett.* **96** 086805 (2006)
20. Lemonik Y et al. *Phys. Rev. B* **82** 201408(R) (2010)
21. Vafek O, Yang K *Phys. Rev. B* **81** 041401(R) (2010)
22. Abanin D A et al. *Science* **332** 328 (2011)
23. McEuen P L et al. *Phys. Rev. Lett.* **64** 2062 (1990)
24. Haug R J *Semicond. Sci. Technol.* **8** 131 (1993)
25. Tombros N et al. *Nature* **448** 571 (2007)
26. Sinova J et al. *Phys. Rev. Lett.* **92** 126603 (2004)
27. Kato Y K *Science* **306** 1910 (2004)
28. Wunderlich J et al. *Phys. Rev. Lett.* **94** 047204 (2005)
29. Imada M, Fujimori A, Tokura Y *Rev. Mod. Phys.* **70** 1039 (1998)
30. Evers F, Mirlin A D *Rev. Mod. Phys.* **80** 1355 (2008)
31. Ponomarenko L A et al. *Nature Phys.* **7** 958 (2011)
32. Katsnelson M I, Novoselov K S, Geim A K *Nature Phys.* **2** 620 (2006)
33. Cheianov V V, Fal'ko V I *Phys. Rev. B* **74** 041403(R) (2006)
34. Adam S et al. *Proc. Natl. Acad. Sci. USA* **104** 18392 (2007)
35. Cheianov V V et al. *Phys. Rev. Lett.* **99** 176801 (2007)

PACS numbers: **42.25.–p**, **42.30.–d**, 42.60.Jf
DOI: 10.3367/UFNe.0182.201204f.0442

Modern optics of Gaussian beams

V G Volostnikov

1. Introduction

A coherent light field, like any oscillatory process, is characterized by its amplitude and phase. The methods and means for analyzing light fields from intensity measurements underlie optical instruments, and from the physical standpoint the solution to any optical measurement problem

V G Volostnikov Samara Branch of the P N Lebedev Physical Institute, Russian Academy of Sciences, Samara, Russian Federation
E-mail: coherent@fian.smr.ru

Uspekhi Fizicheskikh Nauk **182** (4) 442 – 450 (2012)
DOI: 10.3367/UFNr.0182.201204f.0442
Translated by E N Ragozin; edited by A Radzig